

# Radiative leptonic $B$ decays in the instantaneous Bethe-Salpeter approach

G. A. Chelkov<sup>1</sup>, M. I. Gostkin<sup>1</sup> and Z. K. Silagadze<sup>2</sup>

<sup>1</sup> *JINR, Laboratory of Nuclear Problems,  
141 980, Dubna, Russia;*

<sup>2</sup> *Budker Institute of Nuclear Physics,  
630 090, Novosibirsk, Russia;*

## Abstract

Rare radiative leptonic decay  $B \rightarrow l\bar{\nu}_l\gamma$  is studied in the instantaneous Bethe-Salpeter approach. The results are compared to other relativistic quark model predictions.

The  $B$ -meson decay constant  $f_B$  is an important phenomenological parameter, not easy to measure directly. Purely leptonic decays  $B \rightarrow l\bar{\nu}_l$ , from which it could be extracted in principle, suffer either from helicity suppression  $m_l^2/M_B^2$  for light leptons, or from reconstruction difficulties for  $\tau$ -channel owing to the presence of two neutrinos in the final state. Decay rates expected in the Standard Model are

$$\Gamma(B \rightarrow l\bar{\nu}_l) = \frac{G_F^2}{8\pi} |V_{ub}|^2 f_B^2 \frac{m_l^2}{M_B^2} M_B^3 \left(1 - \frac{m_l^2}{M_B^2}\right)^2 \approx \begin{cases} 7 \cdot 10^{-12}, & \text{if } l = e^- \\ 3 \cdot 10^{-7}, & \text{if } l = \mu^- \end{cases}$$

where numbers quoted correspond to  $|V_{ub}| = 3 \cdot 10^{-3}$ ,  $f_B = 200 \text{ MeV}$  and  $\tau_B \approx 1.65 \text{ ps}$ . The present experimental limits [1] on these decay rates are at least an order of magnitude larger.

Some times ago Burdman, Goldman and Wyler (BGW) suggested an alternative, although model-dependent way for  $f_B$  measurement [2]. The crucial observation was that the helicity suppression can be overcome and turned into an  $\alpha$  (the e.m. fine-structure constant) suppression by an additional photon emission in radiative weak decays  $B \rightarrow l\bar{\nu}_l\gamma$ . The dominant contribution in these radiative decays comes from the  $B^*$ -pole intermediate state: a spin-0  $B$  meson emits a hard photon and transforms into an off-shell spin-1  $B^*$  meson which by itself undergoes weak decay without

the helicity suppression. Thus measurement of these decay rates gives a tool to access  $B^*$  meson decay constant  $f_B^*$ . Heavy quark symmetry can be used then to relate  $f_B^*$  and  $f_B$ .

Afterwards  $B \rightarrow l\bar{\nu}_l\gamma$  decay ( up to  $m_l^2/M_B^2$  accuracy the decay rate is independent of the lepton flavor) was considered in a number of publications. The BGW analysis was further refined by Colangelo, De Fazio and Nardulli [3]. It was found, in particular, that the axial-vector ( $B'$ ) intermediate state contributes about 10% in the total decay rate. Atwood, Eilam and Soni used a simple nonrelativistic quark model to estimate the decay width and obtained [4]  $Br(B \rightarrow l\bar{\nu}_l\gamma) \approx 3.5 \cdot 10^{-6}$ , about 12 times larger than the purely leptonic branching ratio  $Br(B \rightarrow \mu\bar{\nu}_\mu)$ . Subsequent relativistic generalizations involve the use of: spinless Salpeter equation [5], light front dynamics [6], light cone QCD sum rules [7], perturbative QCD combined with the heavy quark effective theory [8]. All of them confirm the main conclusion about the radiative decay mode enhancement, although with smaller branching ratio ranging from  $0.9 \cdot 10^{-6}$  [5] to  $2 \cdot 10^{-6}$  [7]. The recent experimental upper limits [9] are still far above of these predictions.

It is worthwhile to note that the photon spectra in various relativistic quark models are significantly different as illustrated by Fig.1. An inverted-parabolic shape from [4], with a mean value  $\sim 1.3GeV$ , is asymmetrically modified in [5, 6] towards higher photon energies, but in opposite direction in the light cone QCD sum rules approach [7], with the mean value shifted down to  $\sim 0.8GeV$ . This softening of the photon spectrum can effect the signal detection efficiency [9, 10] and the signal-background separation. We decided to check whether character of change in the photon energy distribution, predicted in [7], still persists in an another, instantaneous Bethe-Salpeter approach based, relativistic quark model [11, 12, 13], which was successfully applied earlier to describe light [14] and heavy [13, 15] meson spectra, as well as electromagnetic form-factors of the ground state pseudoscalar and vector mesons [16], various two photon widths [17] and heavy meson weak decays [18]. This approach respects the heavy quark spin symmetry in the limit  $m_b \rightarrow \infty$  [13]. It also incorporates the spontaneous breaking of chiral symmetry in the light flavor sector, which happens due to the generation of a dynamical quark mass in the light quark self-energy generated by the interaction potential.

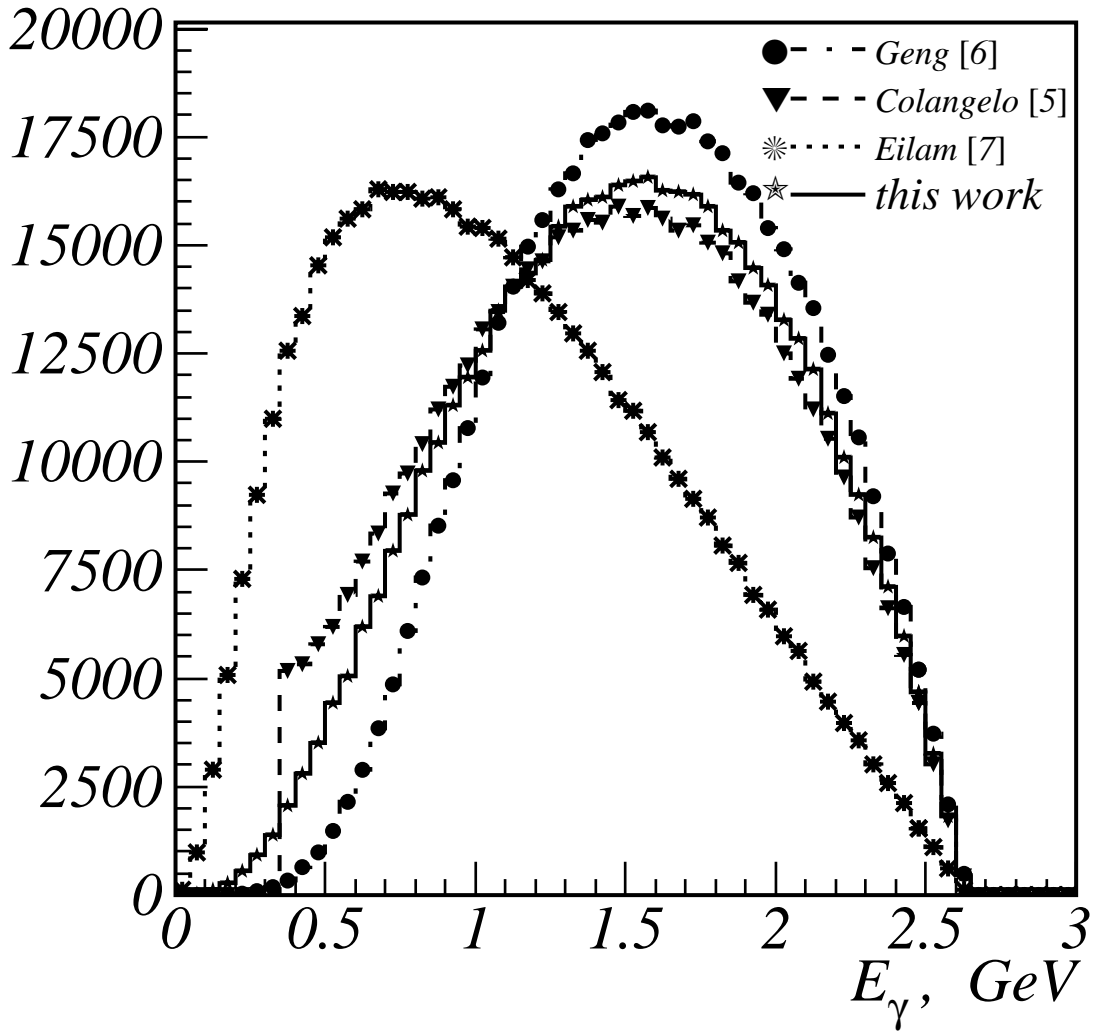


Figure 1: Photon spectra in various relativistic quark models for the  $B \rightarrow l\bar{\nu}_l\gamma$  decay.

The  $B \rightarrow l\bar{\nu}_l\gamma$  matrix element has the following general structure

$$A(B \rightarrow l\bar{\nu}_l\gamma) = \frac{ieG_F V_{ub}}{\sqrt{2}M_B} \epsilon_\nu^* H^{\mu\nu} \bar{u}(p_l) \gamma_\mu (1 - \gamma_5) v(p_\nu) ,$$

where  $H_{\mu\nu}$ , the hadronic tensor, is uniquely determined, due to gauge invariance and Lorentz covariance, by two invariant form-factors  $F_V$  and  $F_A$ :

$$H_{\mu\nu} = F_A [g_{\mu\nu} P \cdot k - k_\mu P_\nu] + iF_V \epsilon_{\mu\nu\sigma\tau} P^\sigma k^\tau \quad (1)$$

$P$  being the  $B$ -meson 4-momentum and  $k$  – the photon 4-momentum (in the following we will assume the  $B$ -meson rest frame in all expressions, so  $P = (M_B, \vec{0})$ ).

The standard procedure leads to the following differential width ( $m_l$  is neglected)

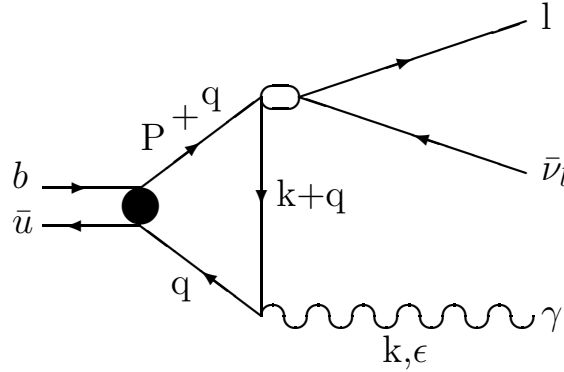
$$\frac{d^2\Gamma}{dx_1 dx_2} =$$

$$M_B \frac{\alpha(G_F M_B^2)^2}{16\pi^2} |V_{ub}|^2 [\rho_+(x_1, x_2) |F_V + F_A|^2 + \rho_-(x_1, x_2) |F_V - F_A|^2] \quad (2)$$

where  $\rho_+(x_1, x_2) = (1-2x_1)(1-2x_2)^2$ ,  $\rho_-(x_1, x_2) = (1-2x_1)(1-2x_3)^2$  and  $x_1 = E_\gamma/M_B$ ,  $x_2 = E_\nu/M_B$ ,  $x_3 = E_l/M_B = 1 - x_1 - x_2$  are the photon, neutrino and charged lepton energy fractions.  $F_V$  and  $F_A$  form-factors depend only on the photon energy, so one integration can be readily done while calculating the decay width, and we get

$$\Gamma(B \rightarrow l \bar{\nu}_l \gamma) = M_B \frac{\alpha(G_F M_B^2)^2}{6\pi^2} |V_{ub}|^2 \int_0^{\frac{1}{2}} x_1^3 (1-2x_1) [ |F_V(x_1)|^2 + |F_A(x_1)|^2 ] dx_1. \quad (3)$$

The photon emission from the initial light quark gives the most important contribution to the  $B \rightarrow l \bar{\nu}_l \gamma$  decay amplitude [4]:



From this diagram the corresponding contribution to the hadronic tensor is easily obtained

$$H_{\mu\nu} = -M_B N_c Q_u \int \frac{dq}{(2\pi)^4} Sp \{ \gamma_\mu (1 - \gamma_5) G_{(b)}(P+q) \Gamma(\vec{q}; P) G_{(u)}(q) \gamma_\nu G_{(u)}(q+k) \}, \quad (4)$$

where  $Q_u = \frac{2}{3}$ ,  $G_{(q)}(p) = \frac{i}{\hat{p} - m_q}$  stands for the constituent  $q$ -quark propagator and  $\Gamma(\vec{q}; P)$  – for the Bethe-Salpeter vertex function [12]. The Mandelstam formalism [19] or the bilocal effective meson theory [20] gives a general guidelines how to calculate transition or decay amplitudes, involving bound states, in terms of this vertex function.

In the instantaneous approximation the Bethe-Salpeter vertex function  $\Gamma(\vec{q}; P)$  depends only on the relative three-momentum  $\vec{q}$  [12]. So the dependence on  $q_0$  in (4) is completely due to quark propagators and the

$q_0$ -integration may be performed analytically using the residue theorem and

$$G_{(q)}(p) = i \left[ \frac{\Lambda_+^{(q)}(\vec{p})}{p_0 - \omega_{(q)}(\vec{p}) + i\epsilon} + \frac{\Lambda_-^{(q)}(\vec{p})}{p_0 + \omega_{(q)}(\vec{p}) - i\epsilon} \right] \gamma^0 ,$$

where  $\omega_{(q)}(\vec{p}) = \sqrt{m_q^2 + \vec{p}^2}$  and  $\Lambda_{\pm}^{(q)}$  are the standard projection operators on positive and negative energies

$$\Lambda_{\pm}^{(q)}(\vec{p}) = \frac{1}{2} \left( 1 \pm \frac{\vec{\alpha} \cdot \vec{p} + \beta m_q}{\omega_{(q)}(\vec{p})} \right) .$$

After  $q_0$ -integration in (4) we obtain several terms, from which the leading contribution comes from the following one

$$H_{\mu\nu} \approx - \int \frac{d\vec{q}}{(2\pi)^3} \frac{M_B N_c Q_u Sp \left\{ \gamma_\mu (1 - \gamma_5) \Gamma_{+-}(\vec{q}; P) \gamma_\nu \Lambda_+^{(u)}(\vec{q} + \vec{k}) \gamma_0 \right\}}{[M_B - \omega_{(b)}(\vec{q}) - \omega_{(u)}(\vec{q})][k_0 - \omega_{(u)}(\vec{q}) - \omega_{(u)}(\vec{q} + \vec{k})]} , \quad (5)$$

because in the heavy  $b$ -quark limit the characteristic momentum scale for  $\Gamma(\vec{q}; P)$  is much less than  $m_b$  and so we may use

$$M_B \approx m_b \approx \omega_{(b)}(\vec{q}) , \quad \omega_{(u)}(\vec{q} + \vec{k}) \approx k_0 \gg \omega_{(u)}(\vec{q}) .$$

In (5)  $\Gamma_{+-}(\vec{q}; P) = \Lambda_+^{(b)}(\vec{q}) \gamma^0 \Gamma(\vec{q}; P) \gamma^0 \Lambda_-^{(u)}(-\vec{q})$  and it can be immediately replaced by the Salpeter wave function  $\Phi(\vec{q})$  according to the Salpeter equation [12, 13]

$$\Gamma_{+-}(\vec{q}; P) = -[M_B - \omega_{(b)}(\vec{q}) - \omega_{(u)}(\vec{q})] \Lambda_+^{(b)}(\vec{q}) \Phi(\vec{q}) \Lambda_-^{(u)}(-\vec{q}) .$$

In the heavy quark limit  $\Phi(\vec{q})$  has the following simple form [13]

$$\Phi(\vec{q}) \approx \frac{l(q)}{q\sqrt{4\pi}} (1 + \gamma_0) \gamma_5 S_{(u)}^{-1}(\vec{q}) , \quad q = |\vec{q}| , \quad (6)$$

where  $l(q)$  obeys the radial Salpeter equation and  $S_{(u)}^{-1}(\vec{q})$  is the inverse of the Foldy-Wouthuysen matrix for  $u$ -quark:

$$S_{(u)}^{-1}(\vec{q}) = \cos \nu_{(u)}(q) - \frac{\vec{q} \cdot \vec{\gamma}}{|\vec{q}|} \sin \nu_{(u)}(q)$$

the Foldy-Wouthuysen angle being determined as follows

$$\cos 2\nu_{(u)}(q) = \frac{m_u}{\omega_{(u)}(\vec{q})} , \quad \sin 2\nu_{(u)}(q) = \frac{|\vec{q}|}{\omega_{(u)}(\vec{q})} .$$

To simplify (5), note also that

$$\Lambda_+^{(u)}(\vec{k} + \vec{q})\gamma_0 = S_{(u)}^{-1}(\vec{k} + \vec{q})\frac{1}{2}(1 + \gamma_0)S_{(u)}(\vec{k} + \vec{q})\gamma_0 = \frac{1}{2}(S_{(u)}^{-2}(\vec{k} + \vec{q}) + \gamma_0).$$

But

$$S_{(u)}^{-2}(\vec{k} + \vec{q}) = \frac{m_u}{\omega_{(u)}(\vec{k} + \vec{q})} - \frac{(\vec{k} + \vec{q}) \cdot \vec{\gamma}}{\omega_{(u)}(\vec{k} + \vec{q})} \approx -\frac{\vec{k} \cdot \vec{\gamma}}{\omega_{(u)}(\vec{k} + \vec{q})}$$

and

$$S_{(u)}^{-2}(\vec{k} + \vec{q}) + \gamma_0 \approx \frac{1}{\omega_{(u)}(\vec{k} + \vec{q})}[\gamma_0 \omega_{(u)}(\vec{k} + \vec{q}) - \vec{k} \cdot \vec{\gamma}] \approx \frac{\hat{k}}{\omega_{(u)}(\vec{k} + \vec{q})}.$$

After these approximations (5) takes manifestly gauge invariant form:

$$H_{\mu\nu} = -\frac{M_B N_c Q_u}{4\sqrt{\pi}} \int \frac{d\vec{q}}{(2\pi)^3} \frac{l(q)}{q} \frac{Sp\{\gamma_\mu(\gamma_5 - 1)(1 - \gamma_0)S_{(u)}^{-1}(\vec{q})\gamma_\nu \hat{k}\}}{\omega_{(u)}(\vec{q})\omega_{(u)}(\vec{k} + \vec{q})}. \quad (7)$$

Now it is straightforward to get  $F_V$  and  $F_A$ , the invariant form-factors from (7) as

$$F_V = F_A = Q_u (f(x_1) + g(x_1)) \quad (8)$$

where (we have introduced  $r = \frac{m_u}{M_B}$  and  $x = \frac{q}{M_B}$  dimensionless variables)

$$f(x_1) = \frac{N_c}{(2\pi)^{5/2}} \frac{1}{x_1} \int_0^\infty l(x) [\varphi(x, x_1) - \varphi(x, -x_1)] \left[ \frac{r + \sqrt{r^2 + x^2}}{\sqrt{r^2 + x^2}} \right]^{1/2} dx$$

$$g(x_1) = \frac{N_c}{(2\pi)^{5/2}} \frac{1}{3x_1^2} \int_0^\infty l(x) [\psi(x, -x_1) - \psi(x, x_1)] \left[ \frac{\sqrt{r^2 + x^2} - r}{\sqrt{r^2 + x^2}} \right]^{1/2} \frac{dx}{x}, \quad (9)$$

and

$$\varphi(x, x_1) = \sqrt{\frac{r^2 + (x + x_1)^2}{r^2 + x^2}}, \quad \psi(x, x_1) = (r^2 + x^2 + x_1^2 - xx_1)\varphi(x_1). \quad (10)$$

Note that in the nonrelativistic (heavy  $u$ -quark, but  $m_u \ll m_b$ ) limit characteristic momentum scale for  $l(x)$  is much less than  $r$ . So  $g(x_1) \rightarrow 0$  and

$$f(x_1) \rightarrow \frac{2\sqrt{2}N_c}{(2\pi)^{5/2}} \frac{1}{x_1 r} \int_0^\infty xl(x)dx.$$

In this limit  $B$ -meson decay constant  $f_B$  takes the form [13]

$$f_B \approx \frac{4\sqrt{2}N_c}{(2\pi)^{5/2}} M_B \int_0^\infty x l(x) dx .$$

So

$$f(x_1) \approx \frac{1}{2x_1} \frac{f_B}{m_u} .$$

Substituting this into (8) and (3), we reproduce Atwood, Eilam and Soni's result [4]

$$\Gamma(B \rightarrow l \bar{\nu}_l \gamma) = M_B \frac{\alpha(G_F M_B^2)^2}{288\pi^2} Q_u^2 |V_{ub}|^2 \frac{f_B^2}{m_u^2} .$$

The equality of the vector and axial current form factors, given by (8), is surprising because in the pole approximation they receive contributions from intermediate states with opposite parities. Nevertheless this additional interesting spin symmetry was shown to hold in the high recoil  $E_\gamma \gg \Lambda_{QCD}$  region at least at one-loop order by explicit leading twist perturbative QCD calculation [8].

The radial wave function  $l(x)$  is determined from the integral equation which in the heavy  $b$ -quark limit takes the form [13]

$$[M - m_b - \omega_{(u)}(p)] l(p) = \frac{1}{2} \int_0^\infty dq \left[ \sqrt{\left(1 + \frac{m_u}{\omega_{(u)}(p)}\right) \left(1 + \frac{m_u}{\omega_{(u)}(q)}\right)} v_0(p, q) + \right. \\ \left. \sqrt{\left(1 - \frac{m_u}{\omega_{(u)}(p)}\right) \left(1 - \frac{m_u}{\omega_{(u)}(q)}\right)} v_1(p, q) \right] l(q), \quad (11)$$

where  $M$  is the bound state mass and  $v_L(p, q)$  angular matrix element of the potential kernel is determined through

$$\frac{pq}{(2\pi)^3} \int d\Omega_p \int d\Omega_q Y_{L'M'}^*(\hat{\vec{p}}) V(\vec{p} - \vec{q}) Y_{LM}(\hat{\vec{q}}) = v_L(p, q) \delta_{LL'} \delta_{MM'} .$$

For estimation purposes we have used the same parameter set for the  $B$ -meson description as given in [13]. That is constituent quark masses  $m_b = 4.79$  GeV,  $m_u = 0.33$  GeV and the linear plus Coulomb potential

$$V(r) = -\frac{4}{3} \frac{\alpha_s}{r} + \sigma^2 r,$$

with  $\alpha_s = 0.39$  and  $\sigma = 0.41$  GeV.

For these parameters the radial Salpeter equation (11) was solved by Mulhopp method [13, 21]. The resulting radial wave function is shown in

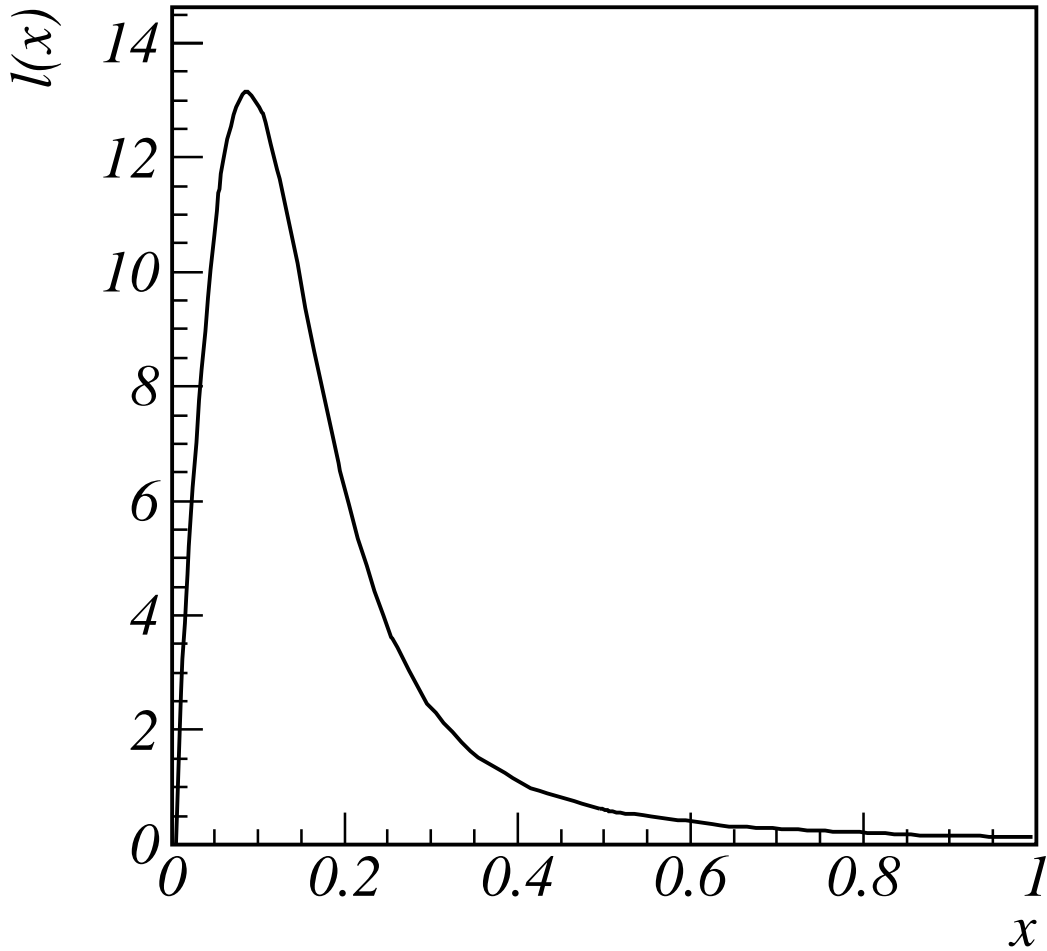


Figure 2: The radial wave function  $l(x)$ .

Fig.2. Note that (11) determines  $l(x)$  only up to normalization constant. The normalization condition was considered for a general case in [13] and for our approximations looks like

$$\frac{N_c}{2\pi^3} \int_0^\infty l^2(x) dx = 1.$$

Having at hand the radial wave function, we can calculate the decay branching ratio

$$Br(B \rightarrow l\bar{\nu}_l\gamma) \approx 0.9 \times 10^{-6}.$$

The resulting photon spectrum is indicated in Fig.1. As one can see, our results are very close to predictions of the spinless Salpeter equation model [5], except in the low-energy part of the photon spectrum where the results of [5] contain unphysical divergence and are not reliable.



To summarize, the instantaneous Bethe-Salpeter model, considered in this article, gives a photon spectrum similar to other relativistic quark models [5] and [6], but different from the light cone QCD sum rules approach [7]. The predicted branching ratio is within the reach of the BaBar experiment [10]. So we may expect that some experimental information will appear about this rare decay mode in the near future. To extract interesting quantities like  $f_B$  from this information, a detailed understanding of the model uncertainties in simulation of this decay is necessary. We hope that our investigation will be useful in such studies.

## Acknowledgement

We thank Fulvia De Fazio and Chao-Qiang Geng for correspondence. The solution of the radial Salpeter equation was provided by Christian Weiss. We gratefully acknowledge this contribution and thank him for critical remarks.

## References

- [1] M. Artuso *et al.* [CLEO Collab.], Phys. Rev. Lett. **75**, 785 (1995).  
D. Buskulic *et al.* [ALEPH Collab.], Phys. Lett. **B343**, 444 (1995).
- [2] G. Burdman, T. Goldman and D. Wyler, Phys. Rev. **D 51**, 111 (1995).
- [3] P. Colangelo, F. De Fazio and G. Nardulli, Phys. Lett. **B372**, 331 (1996).
- [4] D. Atwood, G. Eilam and A. Soni, Mod. Phys. Lett. **A11**, 1061 (1996).
- [5] P. Colangelo, F. De Fazio and G. Nardulli, Phys. Lett. **B386**, 328 (1996);  
F. De Fazio, hep-ph/9609305.
- [6] C. Q. Geng, C. C. Lih and W. Zhang, Phys. Rev. **D 57**, 5697 (1998);  
C. C. Lih, C. Q. Geng and W. Zhang, Phys. Rev. **D 59**, 114002 (1999).
- [7] G. Eilam, I. Halperin and R. R. Mendel, Phys. Lett. **B361**, 137 (1995).
- [8] G. P. Korchemsky, D. Pirjol and T. Yan, Phys. Rev. **D 61**, 114510 (2000);  
D. Pirjol, hep-ph/0101045.

- [9] T. E. Browder *et al.* [CLEO Collab.], Phys. Rev. **D 56**, 11 (1997).
- [10] The BaBar physics book: Physics at an asymmetric B factory, SLAC-R-0504, p. 566. Editors P. F. Harrison and H. R. Quinn [BABAR Collab.].
- [11] J. F. Lagaë, Phys. Rev. **D 45**, 305 (1992).  
M. G. Olsson, S. Veseli and K. Williams, Phys. Rev. **D 52**, 5141 (1995).
- [12] J. Resag, C. R. Münz, B. C. Metsch and H. R. Petry, Nucl. Phys. **A578**, 397 (1994).
- [13] Y. L. Kalinovsky and C. Weiss, Z. Phys. **C63**, 275 (1994).
- [14] B. C. Metsch and H. R. Petry, Acta Phys. Polon. **B27**, 3307 (1996);  
E. Klempt, B. C. Metsch, C. R. Münz and H. R. Petry, Phys. Lett. **B361**, 160 (1995);  
B. Metsch, hep-ph/9712247.
- [15] J. Linde and H. Snellman, Nucl. Phys. **A619**, 346 (1997);  
J. Resag and C. R. Münz, Nucl. Phys. **A590**, 735 (1995).
- [16] C. R. Münz, J. Resag, B. C. Metsch and H. R. Petry, Phys. Rev. **C 52**, 2110 (1995).
- [17] C. R. Münz, Nucl. Phys. **A609**, 364 (1996).
- [18] G. Zoller, S. Hainzl, C. R. Münz and M. Beyer, Z. Phys. **C68**, 103 (1995).
- [19] S. Mandelstam, Proc. Roy. Soc. Lond. **A233**, 248 (1955).
- [20] H. Kleinert, Phys. Lett. **B62**, 429 (1976);  
Y. L. Kalinovsky et al., Few Body Syst. **10**, 87 (1991);  
Y. L. Kalinovsky, L. Kaschluhn and V. N. Pervushin, Fortsch. Phys. **38**, 353 (1990);  
R. T. Cahill, J. Praschifka and C. Burden, Austral. J. Phys. **42**, 161 (1989);  
K. Komachiya and R. Fukuda, Phys. Rev. **D 46**, 2602 (1992).
- [21] S. Boukraa and J. L. Basdevant, J. Math. Phys. **30**, 1060 (1989).